Article

Not peer-reviewed version

Enhancing the Hydrolytic Activity of a Lipase towards Larger Triglycerides through Lid Domain Engineering

Laura Fernandez-Lopez , Sergi Roda , Ana Robles-Martín , Rubén Muñoz-Tafalla , David Almendral , Manuel Ferrer * , Víctor Guallar *

Posted Date: 8 August 2023

doi: 10.20944/preprints202308.0633.v1

Keywords: lipase; lid domain; protein engineering; rational design

Article

Enhancing the Hydrolytic Activity of a Lipase towards Larger Triglycerides through Lid Domain Engineering

Laura Fernandez-Lopez [1,†], Sergi Roda [2,†], Ana Robles-Martín [2,4], Rubén Muñoz-Tafalla [2,4], David Almendral [1], Manuel Ferrer [1,*] and Víctor Guallar [2,3,*]

[1] Instituto de Catalisis y Petroleoquimica (ICP), CSIC, 28049 Madrid, Spain; l.fernandez.lopez@csic.es (L.F.-L.); d.almendral@csic.es (D.A.)
[2] Department of Life Sciences, Barcelona Supercomputing Center (BSC), 08034 Barcelona, Spain; sergi.rodallordes@bsc.es (S.R.); ana.robles@bsc.es (A.R.-M.); ruben.munoz@bsc.es (R.M.-T.)
[3] Institution for Research and Advanced Studies (ICREA), 08010 Barcelona, Spain
[4] Universitat de Barcelona (UB), 08007 Barcelona
* Correspondence: mferrer@icp.csic.es (M.F.); victor.guallar@bsc.es (V.G.)
† These authors contributed equally to this work.

Abstract: Lipases have tremendous potential for industrial use, particularly, those mostly active against water-insoluble substrates, such as triglycerides composed of long-chain fatty acids. However, in most cases, mutants often need to be constructed to achieve optimal performance for such substrates. Protein engineering techniques have been reported as strategies for improving lipase characteristics by introducing specific mutations in the cap domain of esterases or in the lid domain of lipases, or through lid domain swapping. Here, we have improved the lipase character of a lipase, retrieved from the Marine Metagenomics MarRef Database and assigned to the *Actinoalloteichus* genus (WP_075743487.1), through site-directed mutagenesis and by substituting its lid domain (FRGTEITQIKDWLTDA) by the one of *Rhizopus delemar* (previously *Rhizopus oryzae*) lipase (FRGTNSFRSAITDIVF). Results demonstrated that the redesigned mutants gain activity against bulkier triglycerides such as glyceryl tridecanoate and tridodecanoate, olive oil, coconut oil, and palm oil. The absence of a residue in the new lid, present in the original lid, appears to be a key aspect to the increase in lipase character, although full activity recovery is only obtained with lid swapping.

Keywords: lipase; lid domain; protein engineering; rational design

1. Introduction

Ester hydrolases (EC 3.1.-.-) are enzymes responsible for the cleavage and formation of ester bonds [1]. Specifically, those enzymes that carry out the hydrolysis of carboxylic esters into their respective acid and alcohol are known as carboxylic ester hydrolases (EC 3.1.1.1.-). This group is further divided into several subgroups according to the substrates they catalyze [2]. Within the carboxylic ester hydrolases (EC 3.1.1.1.-) are lipases or "true lipases" (EC 3.1.1.3), which are involved in the *in vivo* regulation of the storage and mobilization of fatty acids, fundamental energetic and structural components in cells. Specifically, these enzymes perform the initial hydrolysis step of triacylglycerol or triglyceride to diacylglycerol and fatty acid [3]. The distinction between lipases and esterases has been a subject of continuing controversy. In 1958, it was first postulated that lipases were those proteins that carried out interfacial activation [4].

Interfacial activation is the increase in enzyme activity when substrates change from being soluble in an aqueous medium to an aggregated state (such as an emulsion) due to their insolubility [5]. From the discovery of this phenomenon, the idea that there must be some structural explanation was postulated. In 1990, two lipases, triacylglycerol lipase from the fungus *Rhizomucor miehei* [6] and human pancreatic lipase [7], were crystallized for the first time and allowed the observation of a lid domain covering the active site. It was suggested that the presence of this lid was linked to the previously described interfacial activation and that, therefore, a conformational change of the lid

 doi:10.20944/preprints202308.0633.v1

should occur to expose the active site to the entry of substrates. This hypothesis was subsequently supported by the structural resolution of two lipase complexes, *R. miehei* lipase with ethyl ester n-hexylphosphonate [8] and the complex of human pancreatic lipase and procolipase with mixed micelles of phosphatidylcholine and bile salt [9], where a conformational change of the lid allowing entry of substrates to the active site was observed. In brief, this structural motif is placed over the active site and protects the hydrophobic cavity from the polar solvent when the substrate is absent. In organic-aqueous interphases, the lid domain is opened, allowing the access of the substrate to the active site, and thus, having the lipase in an active conformation [10]. This behavior can be achieved due to the amphipathic nature of the lid domain, where the hydrophilic residues face the solvent, and the hydrophobic ones are towards the catalytic site in the closed conformation. Once the enzyme opens the lid domain, the hydrophobic side helps in binding liposoluble substrates around the active site [10,11]. However, it was later shown that not all lipases carried out this interfacial activation phenomenon. Examples are cutinase from *Fusarium solani* [12], pancreatic phospholipase from guinea pig [13] and lipase from *Pseudomonas aeruginosa* [14], which lacked the lid. Also, the triacylglycerol lipase from *Pseudomonas glumae* [15] and the open form of lipase B from *Candida antarctica* [16], both with a lid, do not show interfacial activation [17].

Whether or not an enzyme exhibits interfacial activation and whether or not it has a lid is not indicative of its belonging to the lipase group [1]. Currently, the accepted distinction between lipases and esterases has to do with substrate specificity, so that esterases hydrolyze esters with a short length in the acyl region and soluble in water, whereas lipases prefer substrates with a long chain in the acyl region and insoluble in water [18]. That said, recent studies demonstrated that the specific residues in the lid domain are extremely correlated with the activity and specificity of lipases [19]. This has been widely proven by different articles on lid engineering where they show how dramatically the activity and specificity of lipases can change [19–26]. Thus, the lid domain is an essential "hot spot" for tailoring lipases toward the user's needs [19] for many applications [27–29].

Here we present the engineering of the lid domain of lipase from the *Actinoalloteichus* genus (NCBI Accession Number: WP_075743487.1) to switch from the hydrolysis of small/medium-chain triglycerides to large-chain ones. To this aim, we used alternative approaches. First, we computationally characterized the lid opening of the wild-type and generated a mutant, achieving activity against glyceryl tridecanoate ($TriC_{10:0}$), as well as coconut, palm and olive oil. Second, we used a lid swapping approach with which we achieved also a significant increase in substrate size hydrolysis.

2. Results

2.1. Lipase target selection

In order to discover novel lipases with activity on large triglycerides, we screened the Marine Metagenomics MarRef Database [30] (https://mmp2.sfb.uit.no/; ca. 4.7 million protein coding sequences) . The sequences were selected by querying the input sequences using DIAMOND BLASTP, using default parameters (percent identity >60%; alignment length >70; e-value < $1e^{-5}$) against the 392-long amino acids (AA) lipase from Rhizopus delemar (UniProt accession number I1BGQ3; molecular mass, 42138 Da; isoelectric point, 7.06), previously referred to as Rhizopus oryzae. Although other lipases available in the databases could have been used as targets, we selected the one from R. delemar because its catalytic center is sheltered by an alpha-helix lid and shows a significant activity on large lipid substrates [31,32] (Table 1). It is a very versatile enzyme that attracted the attention of the several industrial enzyme producers due its broad range of industrial applications for esterification, interesterification and transesterification reactions. A total of 20 sequences were retrieved (e-value from $3.1e^{-14}$ to $1.4e^{-4}$ to I1BGQ3). One such sequence (GenBank accession number, WP_075743487; e-value $2.3e^{-1}$), assigned to a bacterium of the genus Actinoalloteichus, was confirmed to encode a predicted full length 271-amino acid long hydrolase (e-value $2.53e^{-11}$ and 33.6% similarity compared to I1BGQ3) with the needed catalytic residues and domains, and it was selected as target for further investigation. Within the Marine Metagenomics MarRef Database the sequence WP_075743487 originated from a microbiome isolated from marine

Preprints (www.preprints.org) | NOT PEER-REVIEWED | Posted: 8 August 2023 doi:10.20944/preprints202308.0633.v1

sponges in a sea coast area (Norway: Trondheim fjord; ENA BioSample accession SAMN03339750; ENA BioProject accession PRJNA275157) [33].

Table 1. Substrate specificity of enzyme variants investigated in this study.

Triglyceride	Spec. act. (Units/g) WP_075743487.1	Spec. act. (Units/g) Addzyme RD	Spec. act. (Units/g) WP_075743487.1$_{lid}$	Spec. act. (Units/g) WP_075743487.1$_{W89M/L60F}$
$TriC_{3:0}$	960±20	590±80	630±20	550±70
$TriC_{4:0}$	1080±10	1080±90	780±70	640±10
$TriC_{8:0}$	3230±10	13440±60	2330±90	13800±290
$TriC_{10:0}$	580±10	9850±350	2220±60	9220±320
Coconut oil	50±10	6630±180	1460±170	1860±370
Palm oil	0	1300±250	1290±210	1050±20
Olive oil	0	3680±270	1210±20	1760±210

[1] Specific activity (unit/g; mean ± SD of triplicates) for 7 model substrates. Activity was determined at 30 °C and pH 8.0. In brief, the activity towards $TriC_{3:0}$ and $TriC_{4:0}$ was determined using a pH indicator (Phenol Red®) assay [34]; for the other substrates activity was evaluated by the NEFA-Kit. For details see Materials and Methods section. The raw data can be found in the Supplementary Material (Raw Dataset).

2.2. Synthesis, expression, purification and characterization

Once identified, the 271-AA long sequence encoding the wild type enzyme (GeneBank acc. Nr. WP_075743487; molecular mass, 30173 Da; isoelectric point, 5.31) was used as template for gene synthesis, performed as detailed in Materials and Methods. After synthesis a 294-AA long sequence was obtained encoding an enzyme with a molecular mass of 32698 Da and an isoelectric point of 5.40. The soluble His-tagged protein was produced and purified (> 98% using SDS-PAGE analysis; Figure S1) after binding to a Ni-NTA His-Bind resin.

The hydrolytic activity of purified protein (WP_075743487.1) was initially evaluated against a series of triglycerides with different chain lengths, namely, glyceryl tripropionate ($TriC_{3:0}$), tributyrate ($TriC_{4:0}$), trioctanoate ($TriC_{8:0}$), and tridecanoate ($TriC_{10:0}$), as well as coconut oil typically dominated by medium-chain triglycerides of lauric ($TriC_{12:0}$), myristic ($TriC_{14:0}$) and palmitic ($TriC_{16:0}$) acids, olive oil (or triolein) mostly composed by long-chain triglycerides of oleic acid ($TriC_{18:1}$), and palm oil dominated by long-chain triglycerides of palmitic acid ($TriC_{16:0}$) and stearic acid ($TriC_{18:0}$). The protein was found to be active against short ($TriC_{3:0}$ and $TriC_{4:0}$) to medium ($TriC_{10:0}$ and coconut oil) size triglycerides, with specific activities ranging from 50 to 3230 units/g protein, measured at pH 8.0 and 30 °C (Table 1).

The enzyme showed maximal activity at 45 °C, retaining more than 35% of the maximum activity at 30-55 °C (Figure 1A). Analysis by circular dichroism revealed that the enzyme showed a sigmoidal curve with two transitions, one with a denaturation temperature of 46.3 ± 1.8 °C and a second at 82.4 ± 0.2 °C (Figure 1B). The presence of these two phases may therefore indicate the presence of structural elements that may contribute to protein stability and its denaturation under distinct thermal conditions. Its optimal pH for activity is 9.0, retaining more than 50% of the maximum activity at pH from 7.0 to 10.0 (Figure 2).

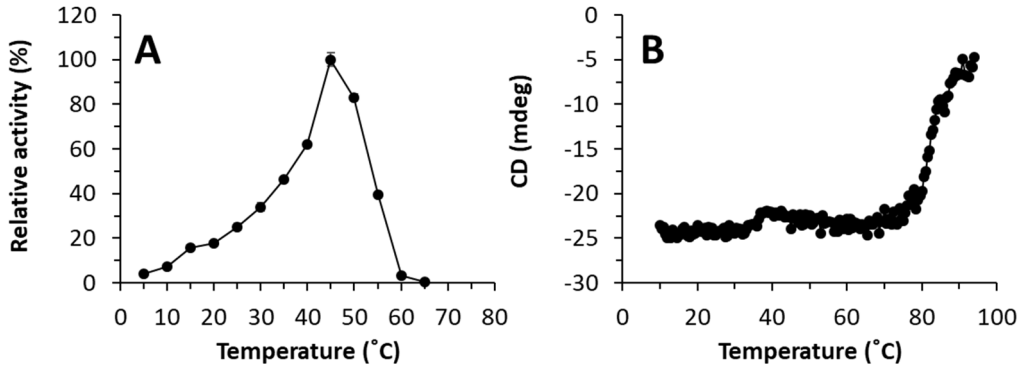

 doi:10.20944/preprints202308.0633.v1

Figure 1. Thermal characteristics of WP_075743487.1. (**A**) Temperature profile. (**B**) The thermal denaturation curve at pH 7.0, as determined by circular dichroism measuring the ellipticity changes at 220 nm obtained at different temperatures at a rate of 0.5 °C per min. In A, the maximal activity was defined as 100% and relative activity is shown as percentage of maximal activity (mean ± SD of triplicates) determined under conditions described in Materials and Methods. The figure was created using Excel 2019. The raw data can be found in the Supplementary Material (Raw Dataset).

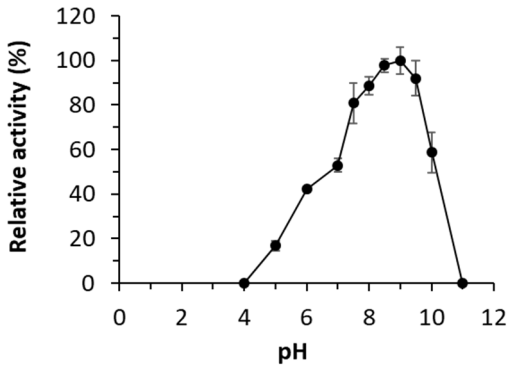

Figure 2. pH profile of WP_075743487.1. The maximal activity was defined as 100%, and relative activity is shown as percentage of maximal activity (mean ± SD of triplicates) determined as described in Materials and Methods. The figure was created using Excel 2019. The raw data can be found in the Supplementary Material (Raw Dataset).

The optimal parameters were in the range of those of the lipase I1BGQ3 used as target for bioprospecting, namely, an optimum pH of 8.5 and an optimum temperature of 30 °C [32]. The substrate specificity of the lipase I1BGQ3 was further evaluated under the same assay conditions herein used to test WP_075743487.1. For that we used the commercial preparation Addzyme RD (Evoxx Technologies GmBH). As shown in Table 1, under our assay conditions this preparation showed a clear preference for the larger triglycerides (specific activities ranging from 590 to 13440 units/g protein), in agreement with previous studies when testing this enzyme with triglycerides from tributyrin to triolein [31,32,35]. Note, that the hydrolase WP_075743487.1 and the lipase Addzyme RD have entirely different specificities with regard their preference for shorter or larger triglycerides, respectively, which may be due to the low similarity between their sequences (about 33%), and possibly between the architecture of their active sites and other structural elements, such as the lid domain as will be discussed below.

2.3. Molecular simulations: reasons for improving the lipase "character"

As shown in Table 1, the enzyme WP_075743487.1 was active towards small-chain triglycerides (glyceryl tributyrate) but had no activity against bulkier triglycerides, under our assay conditions. Since the engineering of the lid domain can lead to drastic changes in the activity and specificity of lipases [19], we visually inspected this structural motif in WP_075743487.1 (Figure 3), to engineer the lid domain to allow the hydrolysis of bulkier triglycerides, we first computationally studied the lid opening of the wild-type enzyme and the R. delemar lipase as a control. Afterwards, we tried to design a mutant based on that analysis.

Preprints (www.preprints.org) | NOT PEER-REVIEWED | Posted: 8 August 2023 doi:10.20944/preprints202308.0633.v1

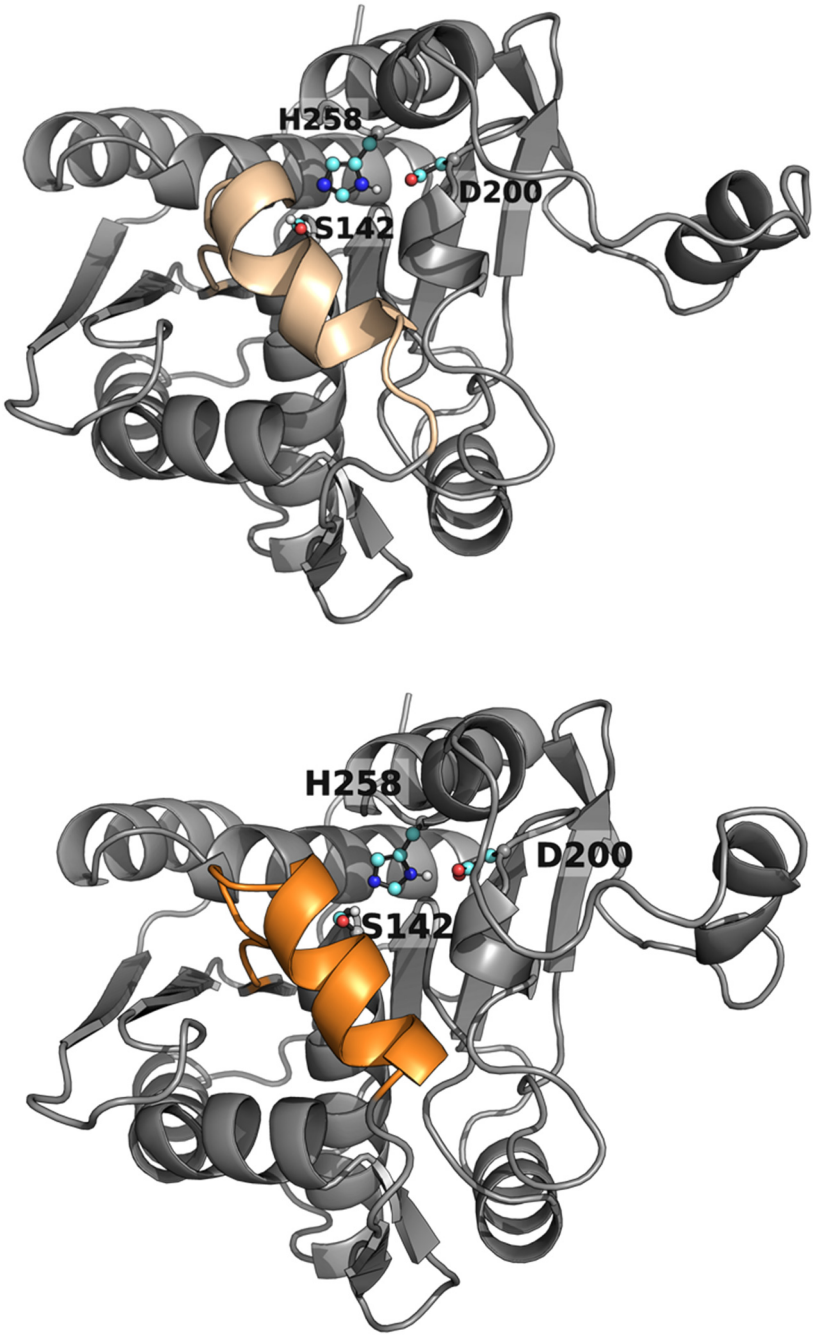

Figure 3. AlphaFold 3D model structure of WP_075743487.1 (top) and WP_075743487.1$_{lid}$ (bottom) highlighting the catalytic triad (with C atoms colored in cyan) and the *lid* domain (colored in wheat and orange, respectively).

The original lid domain (FRGTEITQIKDWLTDA) seemed to have a tryptophan residue at the inner side, hindering its full opening to bind medium and long-chain triglycerides (Figures 4 and S2), in agreement with experimental data (Table 1). Such amino acid is absent in the lid domain FRGTNSFRSAITDIVF of *R. delemar* lipase I1BGQ3 (previously *R. oryzae*, acc. no. P61872) lipase (Figure 4). We performed a molecular simulation with Protein Energy Landscape Exploration (PELE) software [36,37] to check this hypothesis. The simulation consisted of the lipase being solely perturbed by a vector between the α carbons of a residue in the lid domain (I83 for the WP_075743487.1 enzyme and F209 for the *R. delemar* lipase) and a residue in the loop in front of it (L255 for the WP_075743487.1 enzyme and I377 for the *R. delemar* lipase), forcing the opening of the lid domain. After this perturbation of the lid domain, the system was minimized, and the step was

Preprints (www.preprints.org) | NOT PEER-REVIEWED | Posted: 8 August 2023 doi:10.20944/preprints202308.0633.v1

accepted or rejected based on the Metropolis criterion. Moreover, the sense of the vector was changed every 100 steps to study the motion related to the opening and closure of the lid domain and find the metastable opened and closed states.

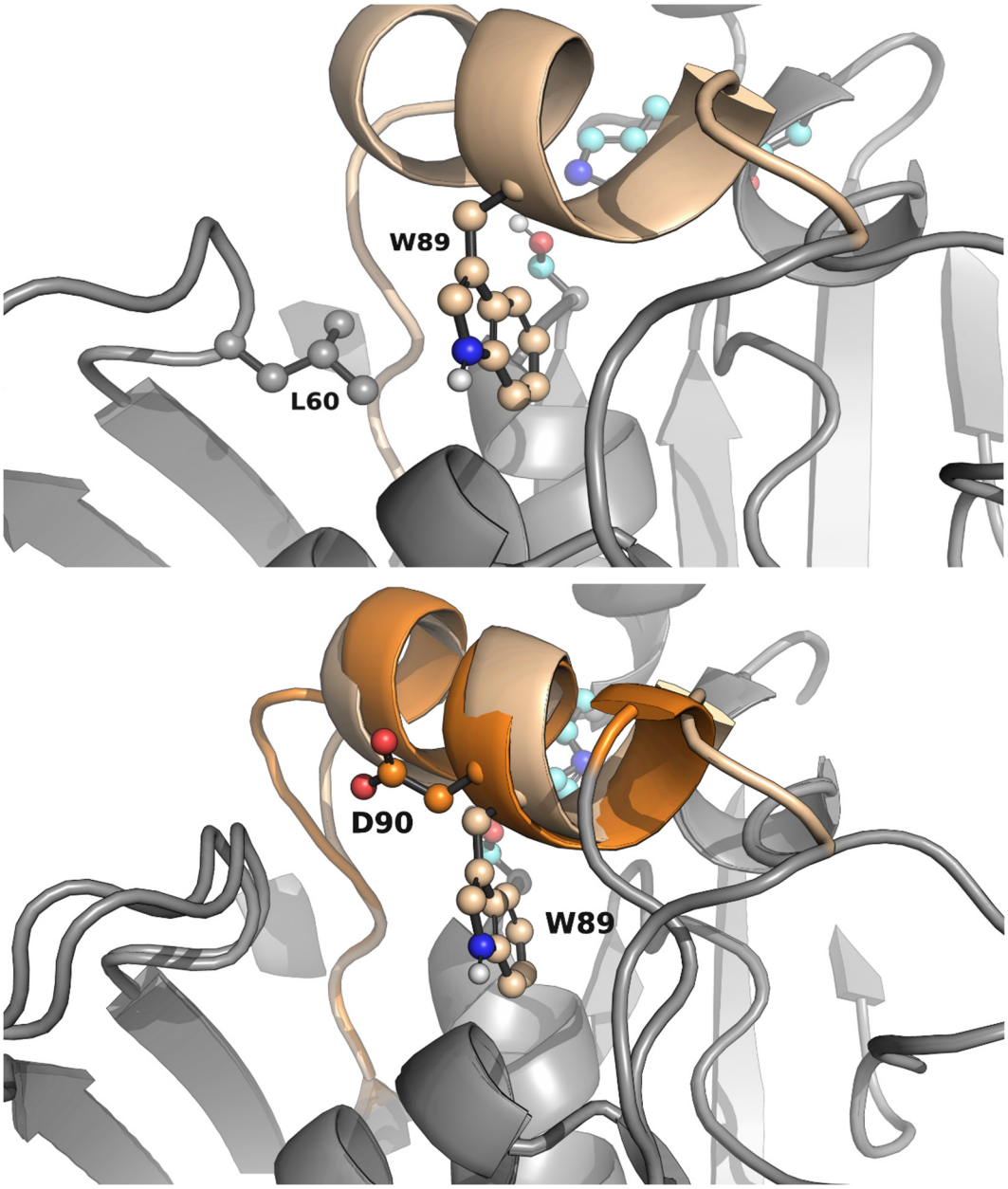

Figure 4. AlphaFold 3D model structure of WP_075743487.1 highlighting the positions of W89 and L60 in the *lid* domain (**top**). AlphaFold 3D model structures of WP_075743487.1 and WP_075743487.1$_{lid}$ depicting the absence of the bulky W residue in the lid domain of the mutant (**bottom**).

The results of the simulations showed that the wild-type enzyme had a closed metastable state at 8.99 Å and an opened one at 14.43 Å, meaning the lid domain opens up to 5.44 Å. On the other hand, the R. delemar lipase had a closed metastable state at 7.71 Å and an opened one at 15.30 Å, showing a difference in the opening distance of 2.14 Å (Figure S3). Thus, we created a variant aiming at opening more the lid domain of the lipase. The designed mutant replaced W89 for a less bulky residue, but still a reasonable change according to the BLOSUM62 matrix, methionine. To compensate for this change and avoid the access of water molecules in the active site to the closed conformation, L60, a residue not placed in the lid domain (Figure 4), was mutated to phenylalanine. Then, the same type of simulation was performed on the double mutant. The results gave a similar

Preprints (www.preprints.org) | NOT PEER-REVIEWED | Posted: 8 August 2023 doi:10.20944/preprints202308.0633.v1

closed metastable conformation (at 8.81 Å), but a more opened one (at 15.78 Å). Thus, the difference in the opening distance between the double mutant and the wild-type was around 1.5 Å, meaning the variant could accommodate bulkier triglycerides (Figure 5).

Local explorations of the binding of triolein (a long-chain triglyceride) in the active state of the wild-type enzyme, the *R. delemar* lipase, and the double mutant (W89M/L60F) were performed to check how the designed lid domain enhanced the catalytic binding of bulkier triglycerides. The ligand was undockable in the open conformation of the wild-type enzyme, so we had to perform a migration of a triolein molecule from the solvent to the active site with AdaptivePELE [36–38] with a bias that allows minimizing the distance between the substrate and the catalytic serine residue. The simulation successfully gave catalytic binding positions of the substrate around the active site (Figure S4). On the other hand, the ligand was easily docked with Glide [39] software on the open conformations of the double mutant and the *R. delemar* lipase (Figure S5). The induced-fit simulations showed that the substrate stays more bound in a catalytic conformation in the double mutant and the *R. delemar* lipase compared to the wild-type enzyme (Figures 6 and S6). Likewise, the wild-type enzyme only had ~56% of PELE poses inside the active site (with the serine-substrate distance equal to or lower than 5 Å), while the double mutant and the *R. delemar* lipase had up to ~82 % and 99 % of them. The number of catalytic events, by meaning of those poses where one of the ester C bonds is at 4 Å from the nucleophile O of the catalytic serine residue, and the H-bonds of the catalytic triad have good distances, is similar in the double mutant, with 1696 (and 10.412 % of all accepted PELE steps) compared to the wild-type enzyme with 2023 (and 12.687 % of all accepted PELE steps) such events. The *R. delemar* lipase showed more catalytic events than the wild-type enzyme with 33604 (and 91.586 % of all accepted PELE steps).

The sequence encoding WP_075743487.1 with the two mutations, W89M and L60F (WP_075743487.1$_{W89M/L60F}$), was synthesized as for the wild-type. After synthesis a 294-AA long sequence was obtained encoding an enzyme with a molecular mass of 32677 Da and an isoelectric point of 5.40. The mutant was expressed, purified, and characterized as for the wild-type protein. The protein was found to be active against small- to medium-length triglycerides, including trioctanoate (TriC$_{8:0}$), but also large triglycerides such as tridecanoate (TriC$_{10:0}$), coconut oil, palm oil and olive oil (Table 1), substrates that the wild-type protein was not able to hydrolyze. Specific activities range from 550 (for TriC$_{3:0}$) to 13800 (for TriC$_{8:0}$) units/g protein, being able to hydrolyze triglycerides as large as olive oil (1760 units/g) and palm oil (1050 units/g). These results agree with computation analysis and the role of the residue W89, located in the original lid domain in the substrate specificity and the access of bulkier triglycerides to the active site. That said, TriC$_{3:0}$ and TriC$_{4:0}$ were found to be the preferred substrates, in this order, for the wild-type. However, the hydrolysis rate was significantly lower for the mutant, namely, about 30 and 10 times in the same order (Table 1).

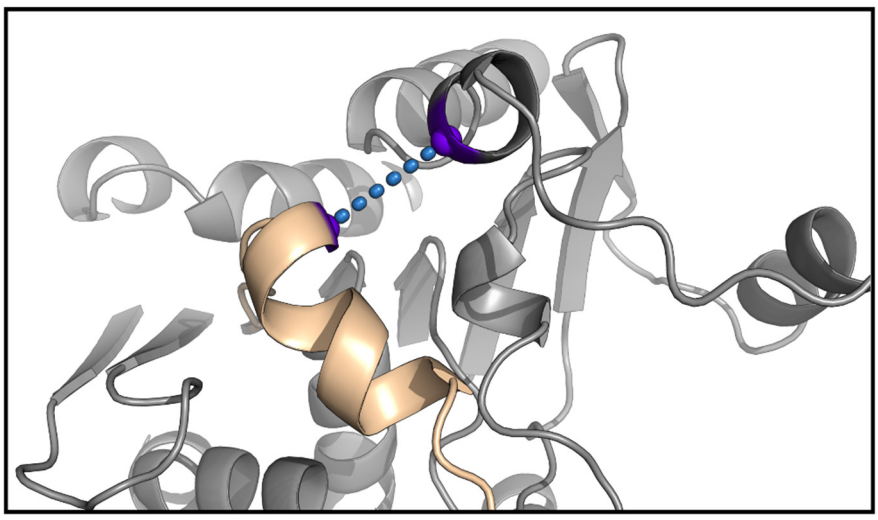

Preprints (www.preprints.org) | NOT PEER-REVIEWED | Posted: 8 August 2023 doi:10.20944/preprints202308.0633.v1

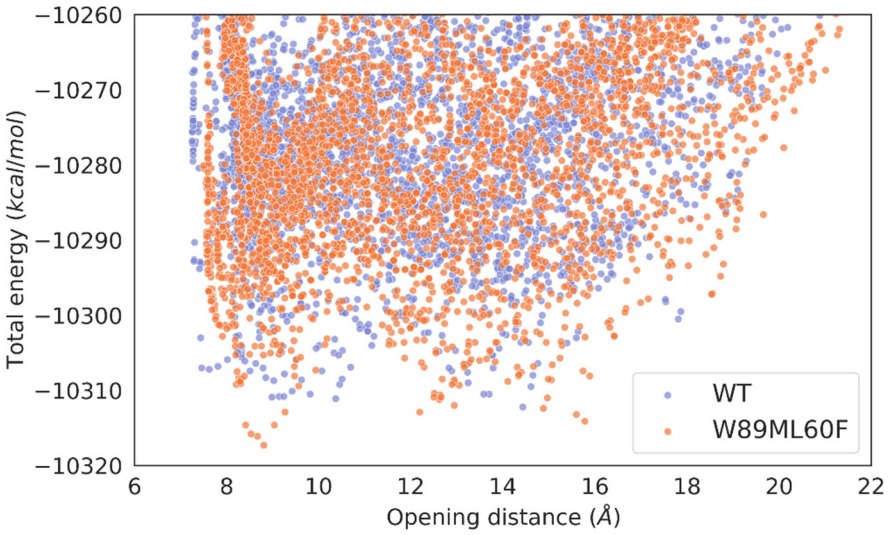

Figure 5. Scatter plots of the opening distance (highlighted on top in the 3D representation) against the total energy of the system. The energy profiles were created with the Matplotlib library [40].

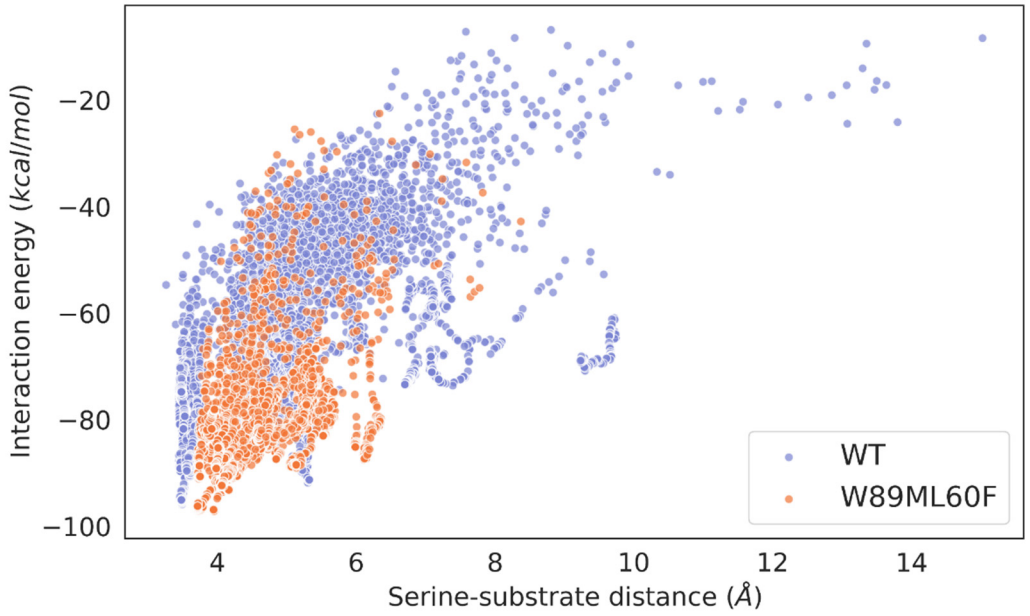

Figure 6. Scatter plots of the serine-substrate (nucleophile O of the catalytic Ser residue and ester Cs of the substrate) distance against the interaction energy of the wild-type and the double mutant. The energy profiles were created with the Matplotlib library [40].

2.4. Molecular simulations: Lid swapping

As a complementary strategy, and based on the results found by mutating a *lid* residue, to further improve the capacity of the lipase to hydrolyze bulkier triglycerides, we performed lid swapping. The lid domain (FRGTEITQIKDWLTDA) of WP_075743487.1 was replaced by the one (FRGTNSFRSAITDIVF) of *R. oryzae* lipase (UniProt accession number I1BGQ3), which was used as template for screening WP_075743487.1 in the Marine Metagenomics MarRef Database, and shares a 33.2% sequence identity in a local sequence alignment and an RMSD of ~ 3 Å with its crystal structure [41] (PDB code: 1TIC, against WP_075743487.1's AlphaFold structure). This enzyme does show an

 doi:10.20944/preprints202308.0633.v1

optimum pH of 8.5 and an optimum temperature of 30 °C [32] and can accept from short ($TriC_{4:0}$) to medium ($TriC_{8:0}$) and large (triolein) triglicerides [31], because its interfacial activation mediated by its hydrophobic amino acids in the lid [41]. The differences in the hydrophobic characters of the lid domains of the two enzymes call into the question whether the lid swapping may improve the lipase character of WP_075743487.1.

First, we also performed the same computational analysis for the new lid swapped mutant, named $WP\_075743487.1_{lid}$ (Figures 3 and 4). The "lid opening" type of simulation for the $WP\_075743487.1_{lid}$ variant showed a closed metastable conformation at 9.40 Å and a more opened one at 19.61 Å, meaning that this variant had the highest opening distance of all interrogated species (Figure S7). The induced-fit simulation of the lid swapped mutant showed that the substrate stays bound in a catalytic conformation ~ 99 % of the time (Figure S8). Moreover, the number of catalytic events was 30392 (and 91.295 % of all accepted PELE steps), the highest compared to the wild-type enzyme and the double mutant, and with similar values to the *R. delemar* lipase.

The engineered $WP\_075743487.1_{lid}$ variant was then synthesized as for the wild-type. After synthesis a 294-AA long sequence was obtained encoding an enzyme with a molecular mass of 32635 Da and an isoelectric point of 5.56. The N-terminal histidine (His) mutant was expressed, purified, and characterized as for the wild-type protein. The protein was found to be active against all triglycerides tested, with specific activities ranging from 630 (for $TriC_{3:0}$) to 2330 (for $TriC_{8:0}$) units/g protein, being able to hydrolyze triglycerides as large as olive oil (1210 units/g) and palm oil (1290 units/g) to an extend similar to that of the $WP\_075743487.1_{W89M/L60F}$ mutant (Table 1).

It should be noted that the two mutants designed in this study showed a preference for long triglycerides similar to that of the model R. delemar lipase (Table 1), although the specific activity values are not comparable as the latter are derived from a non-pure commercial sample (Addzyme RD).

3. Discussion

Understanding the mechanisms that modulate the substrate specificity of ester hydrolases, both esterases and lipases, and in particular the increase of the lipase character in this type of enzymes has been the subject of analysis both in native enzymes and in mutants designed by protein engineering techniques [19–26]. In this sense, many ester hydrolases present a *lid* domain (in the case of lipases) or a cap domain (in the case of some esterases) whose function is to allow the entry of substrates to the active site, which is known as interfacial activation in the case of lipases, with open and closed forms depending on the displacement of this *lid*. It has been observed that the *lid* described in lipases and the cap domain of esterases have a very similar topology, although, in the latter, no biological functionality has been observed. Still, high flexibility of the N-terminal end has been observed [42]. Although, it is not possible to strictly speak of open and closed forms in esterases, in the specific case of some members of the family IV esterases, the opening of the cap domain seems to be a prerequisite for the entry of substrates into the active center, something that is reminiscent of the role of the *lid* in lipases. This occurs, for example, because of the presence in the cap domain of residues that could act as hinges in the opening of the N-terminal part of the cap domain to facilitate the entry of bulky substrates into the active center [42–46]. Because lipases and esterases come from a common ancestor, the high flexibility of the cap domain observed in the latter could be reminiscent of the interfacial activation of lipases.

Modulating by protein engineering the amino acids of the cap domain in a single esterase, and thus the mobility of the cap domain, has allowed to shape the entry of bulkier substrates into the active center and thus alter the substrate specificity of the esterase. These advances have not occurred at the same level in lipases. Indeed, lipases with different residues and characteristics (e.g. hydrophobicity) or the same lipase with specific changes introduced in the *lid*, can show very different activity profiles and specificity. In this study, we have gone further and approached improving the lipase character of a lipase through computational predicted mutagenesis and *lid* swapping. Specifically, by introducing a double mutant, we significantly increased the size of accepted substrates, as well as the activity on medium ones. Moreover, we went further by changing the *lid* of a lipase with little lipase "character" to the *lid* of another enzyme with a reported lipase "character". The results provided in this study demonstrate unequivocally that this method produces

 doi:10.20944/preprints202308.0633.v1

lipases with better characteristics, in terms of broadening the preference or ability to hydrolyze longer and insoluble substrates. Validation of computation predictions reinforces the hypothesis that the differences in the presence of key residues between the original and the swapped lid domains play a major role in the improving lipase "character". It cannot be ruled out that other factors derived from the incorporation of the new lid domain may contribute to the increase in the lipase character of the originating enzyme, as shown by the improved lipase "character" of WP_075743487.1$_{lid}$ mutant compared to WP_075743487.1$_{W89M/L60F}$ mutant.

4. Materials and Methods

4.1. Source and Production of WP_075743487.1, WP_075743487.1$_{lid}$ and WP_075743487.1$_{W89M/L60F}$

The sequences of WP_075743487.1, WP_075743487.1$_{lid}$, and WP_075743487.1$_{W89M/L60F}$ were synthesized by GenScript Biotech (GenScript Biotech, EG Rijswijk, Netherlands) and were codon-optimized to maximize the expression in *E. coli*. The genes were flanked by BamHI and HindIII (stop codon) restriction sites and inserted into a pET-45b(+) expression vector with an ampicillin selection marker (GenScript Biotech, EG Rijswijk, Netherlands), which was further introduced into *E. coli* BL21(DE3). This plasmid, which was introduced into *E. coli* BL21(DE3), supports the expression of N-terminal histidine (His) fusion proteins, with the final amino acid sequences of the synthetic protein being MAHHHHHHVGTGSNDDDDKSPDP-X (where X corresponds to the original sequence of the target enzyme). The soluble N-terminal histidine (His)-tagged proteins were produced and purified (98% purity, as determined by SDS–PAGE analysis using a Mini PROTEAN electrophoresis system, Bio-Rad, Madrid, Spain) at 4 °C after binding to a Ni-NTA His-Bind resin (Merck Life Science S.L.U., Madrid, Spain), as previously described [34], and stored at −20 °C until use at a concentration of 1.5 mg/mL in 40 mM 4-(2-hydroxyethyl)-1-piperazineethanesulfonic acid (HEPES) buffer (pH 7.0). Approximately 10-14 mg of purified proteins were obtained on average from a 1-L culture.

4.2. Source of Rhizopus delemar lipase

Lipase from *Rhizopus delemar* (Addzyme RD) was kindly provided by Evoxx Technologies GmBH (Monheim am Rhein,), Germany. Prior to use, a stock solution of 1 mg/mL in 40 mM 4-(2-hydroxyethyl)-1-piperazineethanesulfonic acid (HEPES) buffer (pH 7.0) as prepared and used for activity tests.

4.3. Substrate specificity

The enzymes (20 μg/ml) were incubated with a stock solution of each of the target esters, TriC$_{8:0}$ (ref. T9126), TriC$_{10:0}$ (ref. CRM44897), coconut oil (re. C1758), palm oil (ref. 70905) and olive oil (ref. O1514) (all provided by Merck Life Science S.L.U., Madrid, Spain), in 100 μl of (4-(2-hydroxyethyl)-1-piperazinepropanesulfonic acid (EPPS) buffer, 5 mM, pH, 8.0; T, 30 °C. The reactions were maintained in 2-ml safe-lock Eppendorf® polypropylene tubes (ref. 0030 120.094, Greiner Bio-One GmbH, Kremsmünster, Austria) in a thermoshaker (model Thermomixer comfort, Eppendorf AG, Hamburg, Germany) at 950 rpm. After 30 min reaction, the hydrolysis was measured by using the NEFA-Kit (FUJIFILM Wako Chemicals Europe GmbH, Neuss, Germany), following the manufacturer's instructions. Briefly, 10 μl of the reaction solution was mixed with 100 μl of NEFA solution 1 in a 96 well plate (ref. 655801, Greiner Bio-One GmbH, Kremsmünster, Austria). Following 6 min incubation at 37 °C, 50 μl of NEFA solution 2 was added, and after 6 min incubation at 30 °C, the samples' absorbance was measured at 550 nm using a Synergy HT Multi Mode Microplate Reader (BioTek Instruments, Winooski, VT, USA), with Gen5 2.00 software. Note: stock solutions were prepared at concentrations of 282.41 mg/ml for TriC$_{8:0}$, 332.92 mg/ml for TriC$_{10:0}$, 460 mg/ml for coconut oil, 431 mg/ml for palm oil and 431 mg/ml for olive oil, in dimethyl sulfoxide (Merck Life Science S.L.U., Madrid, Spain); this corresponds to a 0.6 M of all esters. The final concentration in the reaction assays were 11.29 mg/ml for TriC$_{8:0}$, 13.32 mg/ml for TriC$_{10:0}$, 18.4 mg/ml for coconut oil, and 17.24 mg/ml for palm oil and olive oil. The activity is calculated by determining the absorbance per minute and by using a NEFA standard (oleic acid, ref. 29124-2, Merck Life Science S.L.U., Madrid, Spain) for calibration. One unit of enzyme activity was defined as 1 μmol of acid produced per minute

 doi:10.20944/preprints202308.0633.v1

under the assay conditions. In all cases, all values in triplicate (n=3) were corrected for nonenzymatic transformation, with the absence of activity defined as having at least a twofold background signal.

The activity towards $TriC_{3:0}$ (ref. W328618) and $TriC_{4:0}$ (ref. W222305), whose hydrolysis cannot be followed by the NEFA-Kit was determined using a pH indicator (Phenol Red®) assay [34]. In brief, reactions were performed as follows: [enzyme], 2.8-45.5 µg/ml (depending on the enzyme); [$TriC_{3:0}$ or $TriC_{4:0}$], 4.5 mg/ml; reaction volume, 40 µl (4-(2-hydroxyethyl)-1-piperazinepropanesulfonic acid, EPPS buffer, 5 mM, phenol red (extinction coefficient of phenol red, 8450 $M^{-1}cm^{-1}$), 0.45 mM, pH 8.0; T, 30 °C; assay format, 384-well plates (ref. 781162, Greiner Bio-One GmbH, Kremsmünster, Austria); assay wavelength, 550 nm. Datasets were collected with a Synergy HT Multi-Mode Microplate reader (with Gen5 2.00 software Biotek Instruments, Winooski, VT, USA), with values obtained from the best linear fit using Excel 2019. In all cases, the activity is calculated by determining the absorbance per minute from the generated slopes [34]. One unit (U) of enzyme activity was defined as the amount of enzyme required to transform 1 µmol of substrate in 1 min under the assay conditions. In all cases, all values in triplicate (n=3) were corrected for nonenzymatic transformation, with the absence of activity defined as having at least a twofold background signal [34].

4.4. pH and thermal profiles

The hydrolysis of the model esters p-nitrophenyl butyrate (p-NP butyrate) (ref. N-9876; Merck Life Science S.L.U., Madrid, Spain) was assessed by monitoring the continuous production of 4-nitrophenol at 348 nm (pH-independent isosbestic point, $\varepsilon = 4147\ M^{-1}\ cm^{-1}$), using 0.2 µg total proteins, as reported [34]. In all cases, a Synergy HT Multi-Mode Microplate Reader with Gen5 2.00 software (Biotek Instruments, Winooski, VT, USA) was used. The effect of the pH on the activity was evaluated in 50 mM Britton-Robinson (BR) buffer at pH 4.0–10.0. Note that the BR buffer consists of a mixture of 0.04 M H_3BO_3, 0.04 M H_3PO_4, and 0.04 M CH_3COOH that was titrated to the desired pH with 0.2 M NaOH. Similar assay conditions were used to assay the effects of temperature on p-NP butyrate hydrolysis, but in this case, the reactions were performed at 40 mM HEPES buffer pH 7.0. All reactions were performed in triplicate (n = 3) with control reactions and background signals considered, with the activity calculated by determining the absorbance per minute from the generated slopes, as reported [34].

Circular dichroism (CD) spectroscopy was used to determine the thermal denaturation profile. CD spectra were acquired between 190 and 270 nm with a Jasco J-720 spectropolarimeter equipped with a Peltier temperature controller employing a 0.1-mm cell at 25 °C. Spectra were analyzed, and the denaturation temperature (T_d) values were determined at 220 nm between 10 and 85 °C at a rate of 30 °C per hour in HEPES buffer 40 mM, pH, 7.0. A protein concentration of 1.0 mg ml^{-1} was used. The T_d (and standard deviation of the linear fit) was calculated by fitting the ellipticity (mdeg) at 220 nm at each of the different temperatures using a 5-parameter sigmoid fit with SigmaPlot 14.0 software.

4.5. Protein and chemical preparation for in silico analysis

The lipase from the *Actinoalloteichus* genus structure was obtained using AlphaFold [47]. Then, the obtained structure was prepared and protonated at pH 8.0, the pH at which the experimental assays were performed, using the Protein Preparation Wizard22. The ester compound used was triolein. All substrates were modeled using the OPLS2005 force field [48]. The atomic charges of triolein were calculated with Jaguar [49] using the density functional theory, with a B3LYP-D3 exchange-correlation functional and the polarized double-zeta (pVDZ) basis set.

4.6. Protein Energy Landscape Exploration (PELE) simulations

PELE was used to model the opening of the *lid* domain in the studied lipase, as well as the binding of triolein to the lipase catalytic site. PELE is a Monte Carlo (MC) based algorithm coupled with protein structure prediction methods [36,37]. This MC method starts with the sampling of different microstates by applying small perturbations (translations and rotations) on the ligand. Then, the flexibility of the protein is considered by applying normal modes through the Anisotropic Network Model (ANM)

 doi:10.20944/preprints202308.0633.v1

approach [50]. Once the system has been perturbed, side chains of the residues near the ligand are sampled with a library of rotamers to avoid steric clashes. Finally, a truncated Newton minimization with the OPLS2005 force field [48] is performed, and the new microstate is accepted or rejected according to the Metropolis criterion. The Variable Dielectric Generalized Born Non-Polar (VDGBNP) implicit solvent [51] was applied to mimic the influence of water around the protein.

5. Conclusions

This work provides a rational-based protein engineering approach to improve the capacity of lipases to hydrolyze large water-insoluble triglycerides. This was done by investigating a lipase isolated from the Marine Metagenomics MarRef Database, which contains a lid domain, but it was only capable of hydrolyzing triglycerides up to trioctanoate ($TriC_{8:0}$). To the best of our knowledge, we have engineered the first example of a lipase in which its lid domain has been replaced by that of another lipase capable of degrading large triglycerides. The resulting lid swapped construct could extend the range of triglycerides being hydrolyzed, such as up to palm oil. Lid swapping can help to tune the substrate profiles of lipases towards large-chain fatty esters beyond the tunnel and active site engineering and specific mutations at the lid domain. The results of the present study are complementary to those of a study that has been conducted to convert a lipase into an esterase capable of better hydrolysing water-soluble substrates, by modifying the lid region [52]. We will continue to explore the biocatalytic potential of lipases, other than that herein investigated, by using this approach. Engineering the same lipase with different lid domains or incorporating the same lid domain into different lipase scaffolds may help to explore the versatility and potential of these types of lipase designs.

Supplementary Materials: The following supporting information can be downloaded at the website of this paper posted on Preprints.org, Figure S1: SDS−PAGE analysis of purified WP_075743487.1, WP_075743487.1$_{lid}$ and WP_075743487.1$_{W89M/L60F}$. Figure S2: AlphaFold 3D model structure of R. *delemar* lipase superposed to the WP_075743487.1 structure high-lighting the catalytic triad and the lid domain. Figure S3: Scatter plots of the opening distance against the total energy of the *R. delemar* lipase. Figure S4: Migration simulation of triolein to WP_075743487.1's active site. Figure S5: The used triolein docking pose on the open conformation structure of WP_075743487.1 $_{W89M/L60F}$'s double mutant, *R. delemar* lipase, and lid swapped mutant, highlighting the catalytic triad and the lid domain. Figure S6: Scatter plots of the serine-substrate distance against the interaction energy of the wild-type and the *R. delemar* lipase. Figure S7: Scatter plots of the opening distance against the total energy of the WP_075743487.1$_{lid}$ system. Figure S8: Scatter plots of the serine-substrate distance against the interaction energy of the wild-type and the lid swapped mutant.

Author Contributions: Conceptualization, M.F., V.G. and S.R.; methodology, S.R., A.R., R.M. and L.F-L.; software, S.R., A.R., R.M. and V.G.; validation, L.F-L., D.A., and M.F.; formal analysis, S.R., A.R., R.M. and L.F-L.; investigation, S.R., A.R., R.M. and L.F-L.; resources, V.G. and M.F.; data curation, S.R. and L.F-L.; writing—original draft preparation, S.R., V.G., M.F.; writing—review and editing, S.R., V.G. and M.F.; visualization, S.R. and L.F-L.; supervision, M.F., V.G.; project administration, M.F., V.G.; funding acquisition, M.F., V.G. All authors have read and agreed to the published version of the manuscript.

Funding: This research was funded by the FuturEnzyme Project funded by the European Union's Horizon 2020 Research and Innovation Programme (Grant Agreement No. 101000327), Grants PID2020-112758RB-I00 (M.F.), PDC2021-121534-I00 (M.F.), TED2021-130544B-I00 (M.F.), PID2019-106370RB-I00 (V.G.) from the Ministerio de Ciencia e Innovación, Agencia Estatal de Investigación (AEI) (Digital Object Identifier 10.13039/501100011033), Fondo Europeo de Desarrollo Regional (FEDER) and the European Union ("NextGenerationEU/PRTR"). S. R. thanks the Spanish Ministry of Science and Innovation for a PhD fellowship (FPU19/00608). A.R.M. thanks the Spanish Ministry of Science and Innovation for a PhD fellowship (PRE2020-091825) and the project PID2019-106370RB-I00.

Institutional Review Board Statement: Not applicable.

Informed Consent Statement: Not applicable.

Data Availability Statement: The raw data supporting reported validation results can be found in the Supplementary Material (Raw Dataset).

Acknowledgments: Authors acknowledge Cristina Coscolín (ICP, CSIC) for her support for the preliminary characterization of the pH-profiling.

Conflicts of Interest: The authors declare no conflict of interest.

References

1. Yassine Ben, A.; Verger, R.; Abousalham, A. Lipases or esterases: Does it really matter? Toward a new bio-physico-chemical classification. *Methods in Molecular Biology* (Clifton, N.J.) **2012**, *861*, 31–51. https://doi.org/10.1007/978-1-61779-600-5_2.
2. Bauer T.L.; Buchholz, P.C.F.; Pleiss J. The modular structure of α/β-hydrolases. *FEBS J.* **2020**, *287*, 1035–1053. https://doi.org/10.1111/FEBS.15071.
3. Cerk, I.K.; Wechselberger, L.; Oberer, M. Adipose triglyceride lipase regulation: An overview. *Curr. Protein. Pept. Sci.* **2018**, *19* (2). https://doi.org/10.2174/1389203718666170918160110.
4. Sarda, L.; Desnuelle, P. Action de la lipase pancréatique sur les esters en émulsion. *Biochim. Biophys. Acta* **1958**, *30*, 513–521. https://doi.org/10.1016/0006-3002(58)90097-0.
5. Verger, R. Interfacial activation of lipases: Facts and artifacts. *Trends. Biotechnol.* **1997**, *15*, 32–38. https://doi.org/10.1016/S0167-7799(96)10064-0.
6. Brady, L.; Brzozowski, A.M.; Derewenda, Z.S.; Dodson, E.; Dodson, G.; Tolley, S.; Turkenburg, J.P.; Christiansen, L.; Huge-Jensen, B.; Norskov, L.; Thim., L.; Menge, U. A serine protease triad forms the catalytic centre of a triacylglycerol lipase. *Nature* **1990**, *343*, 767–770. https://doi.org/10.1038/343767A0.
7. Winkler, F.K.; D'Arcy, A.; Hunziker, W. Structure of human pancreatic lipase. *Nature* **1990**, *343*, 771–774. https://doi.org/10.1038/343771A0.
8. Brzozowski, A.M.; Derewenda, U.; Derewenda, Z.S.; Dodson, G.G.; Lawson, D.M.; Turkenburg, J.P.; Bjorkling, F.; Huge-Jensen, B.; Patkar, S.A.; Thim, L. A model for interfacial activation in lipases from the structure of a fungal lipase-inhibitor complex. *Nature* **1991**, *351*, 491–494. https://doi.org/10.1038/351491A0.
9. van Tilbeurgh, H.; Egloff, M.P.; Martinez, C.; Rugani, N.; Verger, R.; Cambillau, C. Interfacial activation of the lipase-procolipase complex by mixed micelles revealed by X-ray crystallography. *Nature* **1993**, *362*, 814–820. https://doi.org/10.1038/362814A0.
10. Barbe, S.; Lafaquière, V.; Guieysse, D.; Monsan, P.; Remaud-Siméon, M.; André I. Insights into lid movements of *Burkholderia cepacia* lipase inferred from molecular dynamics simulations. *Proteins* **2009**, *77*, 509–523. https://doi.org/10.1002/PROT.22462.
11. Reis, P.; Holmberg, K., Watzke, H.; Leser, M.E.; Miller, R. Lipases at interfaces: A review. *Adv. Colloid Interface Sci*. **2009**, *147–148* (C): 237–250. https://doi.org/10.1016/J.CIS.2008.06.001.
12. Martinez, C.; De Geus, P.; Lauwereys, M.; Matthyssens, G.; Cambillau, C. *Fusarium solani* cutinase is a lipolytic enzyme with a catalytic serine accessible to solvent. *Nature* **1992**, *356*, 615–618. https://doi:10.1038/356615a0.
13. Hjorth, A.; Carrière, F.; Cudrey, C.; Wöldike, H.; Boel, E.; Lawson, D.M.; Ferrato, F.; Cambillau, C.; Dodson, G.G.; Thim, L.; Verger, R. A structural domain (the lid) found in pancreatic lipases is absent in the guinea pig (phospho)lipase. *Biochemistry* **1993**, *32*, 4702–4707. https://doi.org/10.1021/BI00069A003.
14. Jaeger, K.E.; Ransac, S.; Koch, H.B.; Ferrato, F.; Dijkstra, B.W. Topological characterization and modeling of the 3D structure of lipase from *Pseudomonas aeruginosa*. *FEBS Lett.* **1993**, *332*, 143–149. https://doi.org/10.1016/0014-5793(93)80501-K.
15. Noble, M.E.; Cleasby, A.; Johnson, L.N.; Egmond, M.R.; Frenken, L.G. The Crystal structure of triacyl-glycerol lipase from *Pseudomonas glumae* reveals a partially redundant catalytic aspartate. *FEBS Lett*. **1993**, *331*, 123–128. https://doi.org/10.1016/0014-5793(93)80310-Q.
16. Uppenberg, J.; Hansen, M.T.; Patkar, S.; Jones, T.A. The Sequence, crystal structure determination and refinement of two crystal forms of lipase B from *Candida antarctica*. *Structure* **1994**, *2*, 293–308. https://doi.org/10.1016/S0969-2126(00)00031-9.
17. Pandey, S.; Rai, R.; Rai, L.C. Proteomics combines morphological, physiological and bio-chemical attributes to unravel the survival strategy of *Anabaena* sp. PCC7120 under arsenic stress. *J. Proteomics* **2012**, *75*, 921–937. https://doi.org/10.1016/j.jprot.2011.10.011.
18. Ferrer, M.; Bargiela, R.; Martínez-Martínez, M.; Mir, J.; Koch, R.; Golyshina, O.V.; Golyshin, P.N. Biodiversity for biocatalysis: a review of the α/β-hydrolase fold superfamily of esterases-lipases discovered in metagenomes. *Biocatal. Biotransform.* **2015**, *3*, 235–249. https://doi.org/10.3109/10242422.2016.1151416.
19. Khan, F.I.; Lan, D.; Durrani, R.; Huan, W.; Zhao, Z.; Wang, Y. The lid domain in lipases: structural and functional determinant of enzymatic properties. *Front. Bioeng. Biotechnol*. **2017**, *5*, 247303. https://doi.org/10.3389/FBIOE.2017.00016/BIBTEX.

20. Dugi, K.A.; Dichek, H.L.; Santamarina-Fojo, S. Human hepatic and lipoprotein lipase. The loop covering the catalytic site mediates lipase substrate specificity. *J. Biol. Chem.* **1995**, *270*, 25396–25401. https://doi.org/10.1074/jbc.270.43.25396.
21. Pleiss, J.; Fischer, M.; Schmid, R.D. Anatomy of lipase binding sites: The scissile fatty acid binding site." *Chem. Phys. Lipids* **1998**, *93*, 67–80. https://doi.org/10.1016/S0009-3084(98)00030-9.
22. Brocca, S.; Secundo, F.; Ossola, M.; Alberghina, L.; Carrea, G.; Lotti, M. Sequence of the lid affects activity and specificity of *Candida rugosa* lipase isoenzymes. *Protein Sci.* 2003, *12*, 2312. https://doi.org/10.1110/PS.0304003.
23. Santarossa, G.; Lafranconi, P.G.; Alquati, C.; DeGioia, L.; Alberghina, L.; Fantucci, P.; Lotti, M. Mutations in the 'lid' region affect chain length specificity and thermostability of a *Pseudomonas fragi* lipase. *FEBS Lett*. **2005**, *579*, 2383–2386. https://doi.org/10.1016/J.FEBSLET.2005.03.037.
24. Karkhane, A.A.; Yakhchali, B.; Jazii, F.R.; Bambai, B. The effect of substitution of phe181 and phe182 with ala on activity, substrate specificity and stabilization of substrate at the active site of *Bacillus thermocatenulatus* lipase. *J. Mol. Catal., B Enzym.* **2009**, *61*, 162–167. https://doi.org/10.1016/J.MOLCATB.2009.06.006.
25. Kourist, R.; Brundiek, H.; Bornscheuer, U.T. Protein engineering and discovery of lipases. *Eur. J. Lipid Sci. Technol.* **2010**, *112*, 64–74. https://doi.org/10.1002/EJLT.200900143.
26. Panizza, P.; Cesarini, S.; Diaz, P.; Rodríguez Giordano, S. Saturation mutagenesis in selected amino acids to shift *Pseudomonas* sp. acidic lipase lip i.3 substrate specificity and activity. *Chem. Commun. (Camb)* **2014**, *51*, 1330–1333. https://doi.org/10.1039/C4CC08477B.
27. Houde, A.; Kademi, A.; Leblanc, D. Lipases and their industrial applications: An overview. *Appl. Biochem. Biotechnol*. **2004**, *118*, 155–170. https://doi.org/10.1385/ABAB:118:1-3:155.
28. Bornscheuer, U.T.; Kazlauskas, R.J. Hydrolases in organic synthesis: Regio- and stereoselective biotransformations, 2nd Edition. Wiley-VCH Verlag GmbH & Co. KGaA, 2006, pp. 61-140.
29. Hasan, F.; Shah, A.A.; Hameed, A. Industrial applications of microbial lipases. Enzyme Microb. Technol.2006, 39, 235–251. https://doi.org/10.1016/J.ENZMICTEC.2005.10.016.
30. Klemetsen, T.; Raknes, I.A.; Fu, J.; Agafonov, A.; Balasundaram, S.V.; Tartari, G.; Robertsen, E.; Willassen, N.P. The MAR databases: development and implementation of databases specific for marine metagenomics. *Nucleic Acids Res*. **2018**, *46(D1)*, D692–D699. https://doi:10.1093/nar/gkx1036.
31. Kohno, M.; Funatsu, J.; Mikami, B.; Kugimiya, W.; Matsuo, T.; Morita, Y. The crystal structure of lipase II from *Rhizopus niveus* at 2.2 A resolution. *J. Biochem*. **1996**, *120*, 505–510. https://doi:10.1093/oxfordjournals.jbchem.a021442.
32. Beer, H.D.; McCarthy, J.E.; Bornscheuer, U.T.; Schmid, R.D. Cloning, expression, characterization and role of the leader sequence of a lipase from *Rhizopus oryzae*. *Biochim. Biophys. Acta* **1998**, *1399*, 173–180. https://doi:10.1016/s0167-4781(98)00104-3.
33. Nouioui, I.; Rückert, C.; Willemse, J.; van Wezel, G.P.; Klenk, H.P.; Busche, T.; Kalinowski, J.; Bredholt, H.; Zotchev, S.B. Acti-noalloteichus fjordicus sp. nov. isolated from marine sponges: phenotypic, chemotaxonomic and genomic charac-terisation. *Antonie Van Leeuwenhoek* **2017**, *110*, 1705–1717. https://doi:10.1007/s10482-017-0920-9.
34. Roda, S.; Fernandez-Lopez, L.; Benedens, M.; Bollinger, A.; Thies, S.; Schumacher, J.; Coscolín, C.; Kazemi, M.; Santiago, G.; Gertzen, C.G.W.; Gonzalez-Alfonso, J.L.; Plou, F.J.; Jaeger, K.E.; Smits, S.H.J.; Ferrer, M.; Guallar, V. A Plurizyme with transaminase and hydrolase activity catalyzes cascade reactions. *Angew. Chem. Int. Ed. Engl.* **2022**, *61*, e202207344. https://doi.org/10.1002/ANIE.202207344.
35. Klein, R.R.; King, G.; Moreau, R.A.; Haas, M.J. Altered acyl chain length specificity of *Rhizopus delemar* lipase through mutagenesis and molecular modeling. *Lipids* **1997**, *32*, 123–130. https://doi:10.1007/s11745-997-0016-1.
36. Borrelli, K.W.; Vitalis, A.; Alcantara, R.; Guallar, V. PELE: Protein Energy Landscape Exploration. A novel Monte Carlo based technique." J Chem Theory Comput 2005, 1, 1304–1311. https://doi.org/10.1021/CT0501811.
37. Municoy, M.; Roda, S.; Soler, D.; Soutullo, A.; Guallar. V. AquaPELE: A Monte Carlo-based Algorithm to sample the effects of buried water molecules in proteins. *J. Chem. Theory Comput*. **2020**, *16*, 7655–7670. https://doi.org/10.1021/ACS.JCTC.0C00925.
38. Lecina, D.; Gilabert, J.F.; Guallar, V. Adaptive simulations, towards interactive protein-ligand modeling. *Sci. Rep*. **2017**, *7*, 1–11. https://doi.org/10.1038/s41598-017-08445-5.

39. Friesner, R.A.; Banks, J.L.; Murphy, R.B.; Halgren, T.A.; Klicic, J.J.; Mainz, D.T.; Repasky, M.P.; Knoll, E.H.; Shelley, M.; Perry, J.K.; Shaw, D.E.; Francis, P.; Shenkin, P.S. Glide: a new approach for rapid, accurate docking and scoring. 1. Method and assessment of docking accuracy. *J. Med. Chem*. **2004**, *47*, 1739–1749. https://doi.org/10.1021/JM0306430.
40. Hunter, J.D. Matplotlib: A 2D graphics environment. *Comput. Sci. Eng*. **2007**, *9*, 90–95. https://doi.org/10.1109/MCSE.2007.55.
41. Derewenda, U.; Swenson, L.; Wei, Y.; Green, R.; Kobos, P.M.; Joerger, R.; Haas, M.J.; Derewenda, Z.S. Conformational lability of lipases observed in the absence of an oil-water interface: crystallographic studies of enzymes from the fungi *Humicola lanuginosa* and *Rhizopus delemar*. *J. Lipid Res.* **1994**, *35*, 524–534. https://doi.org/10.1016/S0022-2275(20)41203-9.
42. De Simone, G.; Mandrich, L.; Menchise, V.; Giordano, V.; Febbraio, F.; Rossi, M.; Pedone, C.; Manco, G. A substrate-induced switch in the reaction mechanism of a thermophilic esterase: kinetic evidences and structural basis. *J. Biol. Chem*. **2004**, *279*, 6815–23. https://doi.org/10.1074/JBC.M307738200.
43. De Simone, G.; Galdiero, S.; Manco, G.; Lang, D.; Rossi, M.; Pedone, C. A snapshot of a transition state analogue of a novel thermophilic esterase belonging to the subfamily of mammalian hormone-sensitive lipase. *J. Mol. Biol*. **2000**, *303*, 761–771. https://doi.org/10.1006/JMBI.2000.4195.
44. Mandrich, L.; Menchise, V.; Alterio, V.; De Simone, G.; Pedone, C.; Rossi, M.; Manco, G. Functional and structural features of the oxyanion hole in a thermophilic esterase from *Alicyclobacillus acidocaldarius*. *Proteins* **2008**, *71*, 1721–1731. https://doi.org/10.1002/PROT.21877.
45. Höppner, A.; Bollinger, A.; Kobus, S.; Thies, S.; Coscolín, C.; Ferrer, M.; Jaeger, K.E.; Smits, S.H.J. Crystal structures of a novel family IV esterase in free and substrate-bound form. *FEBS J.* **2021**, *288*, 3570–3584. https://doi.org/10.1111/FEBS.15680.
46. Distaso, M.; Cea-Rama, I.; Coscolín, C.; Chernikova, T.N.; Tran, H; Ferrer, M.; Sanz-Aparicio, J.; Golyshin, P.N. The mobility of the cap domain is essential for the substrate promiscuity of a family iv esterase from *Sorghum* rhizosphere microbiome. *Appl. Environ. Microbiol*. **2023**, *89*, e0180722. https://doi.org/10.1128/AEM.01807-22.
47. Jumper, J.; Evans, R.; Pritzel, A.; Green, T.; Figurnov, M.; Ronneberger, O.; Tunyasuvunakool, K.; Bates, R.; Žídek, A.; Potapenko, A.; Bridgland, A.; Meyer, C.; Kohl, S.A.A.; Ballard, A.J.; Cowie, A.; Romera-Paredes, B.; Nikolov, S.; Jain, R.; Adler, J.; Back, T.; Petersen, S.; Reiman, D.; Clancy, E.; Zielinski, M.; Steinegger, M.; Pacholska, M.; Berghammer, T.; Bodenstein, S.; Silver, D.; Vinyals, O.; Senior, A.W.; Kavukcuoglu, K.; Kohli, P.; Hassabis, D. Highly accurate protein structure prediction with AlphaFold. *Nature* **2021**, *596*, 583–589. https://doi.org/10.1038/s41586-021-03819-2
48. Banks, J.L.; Beard, H.S.; Cao, Y.; Cho, A.E.; Damm, W.; Farid, R.; Felts, A.K.; Halgren, T.A.; Mainz, D.T.; Maple, J.R.; Murphy, R.; Philipp, D.M.; Repasky, M.P.; Zhang, L.Y.; Berne, B.J.; Friesner, R.A.; Gallicchio, E.; Levy, R.M. Integrated modeling program, Applied Chemical Theory (IMPACT). *J. Comput. Chem*. **2005**, *26*, 1752–1780. https://doi.org/10.1002/JCC.20292.
49. Ilatovskiy, A.V.; Abagyan, R.; Kufareva, I. Quantum mechanics approaches to drug research in the era of structural chemogenomics. *Int. J. Quantum Chem*. **2013**, *113*, 2110–2142. https://doi: 10.1002/qua.24400
50. Atilgan, A.R.; Durell, S.R.; Jernigan, R.L.; Demirel, M.C.; Keskin, O.; Bahar, I. Anisotropy of fluctuation dynamics of proteins with an elastic network model. *Biophys. J.* **2001**, *80*, 505–515. https://doi.org/10.1016/S0006-3495(01)76033-X.
51. Bashford, D.; Case, D.A. Generalized born models of macromolecular solvation effects. *Annu. Rev. Phys. Chem.* **2000**, *51*, 129–152. https://doi.org/10.1146/ANNUREV.PHYSCHEM.51.1.129.
52. Yu, X.W.; Zhu, S.S.; Xiao, R.; Xu, Y. Conversion of a *Rhizopus chinensis* lipase into an esterase by lid swapping. *J. Lipid Res.* **2014**, *55*, 1044–1051. https://doi:10.1194/jlr.M043950.